CHIN. PHYS. LETT. Vol. 35, No. 9 (2018) 093201

Experimental Study on Double Resonance Optical Pumping Spectroscopy in a Ladder-Type System of ^{87}Rb Atoms *

Yi-Hong Li(李一鸿)[1], Shao-Hua Li(李少华)[1], Jin-Peng Yuan(元晋鹏)[1,2**], Li-Rong Wang(汪丽蓉)[1,2**], Lian-Tuan Xiao(肖连团)[1,2], Suo-Tang Jia(贾锁堂)[1,2]

[1]*State Key Laboratory of Quantum Optics and Quantum Optics Devices, Institute of Laser Spectroscopy, Shanxi University, Taiyuan 030006*

[2]*Collaborative Innovation Center of Extreme Optics, Shanxi University, Taiyuan 030006*

(Received 22 May 2018)

Double resonance optical pumping spectroscopy has an outstanding advantage of high signal-to-noise ratio, thus having potential applications in precision measurement. With the counter propagated 780 nm and 776 nm laser beams acting on a rubidium vapor cell, the high resolution spectrum of $5S_{1/2} - 5P_{3/2} - 5D_{5/2}$ ladder-type transition of ^{87}Rb atoms is obtained by monitoring the population of the $5S_{1/2}$ ground state. The dependence of the spectroscopy lineshape on the probe and coupling fields are comprehensively studied in theory and experiment. This research is helpful for measurement of fundamental physical constants by high resolution spectroscopy.

PACS: 32.10.Fn, 32.70.Fw, 32.70.Jz DOI: 10.1088/0256-307X/35/9/093201

High resolution spectroscopy has been attracting attention for applications in laser frequency stabilization,[1] atomic clock,[2] fundamental physics measurement,[3] and other fields.[4,5] For the high resolution spectroscopy of alkali atoms, the Doppler background hinders the potential applications in laser frequency stabilization and optical communication. To obtain a highly resolved Doppler free spectroscopy, various experimental schemes were employed, such as the optical-optical double resonance spectroscopy,[6] electromagnetically induced transparency spectroscopy,[7] and double resonance optical pumping (DROP) spectroscopy.[8] Compared with other spectroscopy methods, DROP spectroscopy has the remarkable character of a high signal-to-noise ratio for detecting the ground state population instead of the excited state. Since the intermediate state has a strong spontaneous emission rate, which will accelerate the double resonance pumping process, the resolution of the spectroscopy will be increased.

DROP spectroscopy was firstly introduced by Moon *et al.*, they used the $5S_{1/2} - 5P_{3/2} - 4D_{3/2}$ and the $5S_{1/2} - 5P_{3/2} - 4D_{5/2}$ transitions for frequency stabilization of 1.5 μm laser,[8] measured the absolute frequency of the $5S_{1/2} - 5P_{3/2} - 4D_{5/2}$ transition with a femtosecond frequency comb in ^{87}Rb,[9] also measured the hyperfine structure constants of the $5S_{1/2} - 5P_{3/2} - 4D_{3/2}$ transition of ^{85}Rb and ^{87}Rb.[10] Wang *et al.* measured the hyperfine structure constants of the $4D_{5/2}$ state for ^{87}Rb and ^{85}Rb,[11] and stabilized the laser frequency using the DROP spectroscopy of the $6S_{1/2} - 6P_{3/2} - 8S_{1/2}$ transition of cesium.[12] Talker *et al.* used the DROP spectroscopy for stabilizing the frequency of a laser with the hyperfine structure of the $5S_{1/2} - 5P_{3/2} - 4D_{5/2}$ transition in a millimeter-size cell of ^{85}Rb.[13] Becerra *et al.* used the DROP spectroscopy for a nondegenerate four-wave mixing experiment of diamond configuration energy levels in rubidium vapor.[14]

Previous researches mainly focused on the $5S_{1/2} - 5P_{3/2} - 4D_{3/2,5/2}$ transition. Recently, the distinct merits of the $5S_{1/2} - 5P_{3/2} - 5D_{5/2}$ transition have attracted tremendous interest from researchers. The small energy difference between these two transitions induces a high-transition probability and a better Doppler free background. The relatively narrow natural linewidth and lower sensitivity to the external environment make the state a good candidate for establishing optical frequency standards with high stability.[2] In our previous work, we have studied the hyperfine transition spectroscopy of the ^{85}Rb $5D_{5/2}$ state using an optical frequency comb and a continuous-wave laser, the results promoted the research of a higher resolution two-photon spectroscopy.[15,16] Also, the high-resolution spectrum under the optimized parameters shows great potential in determination of the hyperfine structure constants.[17]

In this Letter, we thoroughly investigate the DROP spectroscopy of the $5S_{1/2} - 5P_{3/2} - 5D_{5/2}$ transition. The high resolution DROP spectrum is performed by the 780 nm and 776 nm laser beams acting

*Supported by the National Key R&D Program of China under Grant No 2017YFA0304203, the National Natural Science Foundation of China under Grant Nos 61575116, 61705122, 61728502, 91736209 and 11434007, the Changjiang Scholars and Innovative Research Team in University of Ministry of Education of China under Grant No IRT13076, the Program for Sanjin Scholars of Shanxi Province, the Applied Basic Research Project of Shanxi Province under Grant No 201701D221004, and the Fund for Shanxi '1331 Project' Key Subjects Construction.

**Corresponding author. Email: yjp@sxu.edu.cn; wlr@sxu.edu.cn

© 2018 Chinese Physical Society and IOP Publishing Ltd

on the rubidium vapor cell with counter propagating configuration. The dependences of the spectrum lineshape on variable parameters of different combinations of the laser polarization, the power of the coupling laser, and the probe laser are studied in both theory and experiment. By the comparison of the theoretical results with the experimental ones, we can obtain the clear physical essence of the DROP spectroscopy. This study is important for the application of the DROP spectroscopy in precision measurement.

The experimental setup and related energy levels are shown in Fig. 1. A ladder-type coherent atomic system is employed in this study, which contains an excitation from a ground state $5S_{1/2}$ to a high state $5D_{5/2}$ via an intermediate state $5P_{3/2}$, as shown in Fig. 1(a).

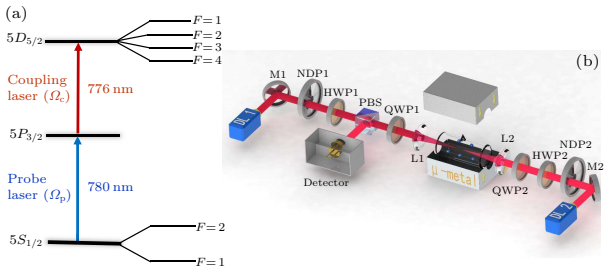

Fig. 1. (a) Relevant energy levels of $5S_{1/2}-5P_{3/2}-5D_{5/2}$ transition of ^{87}Rb. (b) Experimental setup. HWP, half-wave plate; QWP, quarter-wave plate; PBS, polarizing beam splitter; M, high reflection mirror; NDP, neutral density plate; L, lens.

The experimental setup for the DROP spectroscopy is shown in Fig. 1(b). Two tunable Littrow external-cavity diode lasers (DL pro, Toptica) are used as the coupling laser and the probe laser, each operating in a single mode and counter propagate through the Rb vapor cell. The probe laser labeled as DL 1 operating at 780 nm related to the $5S_{1/2}-5P_{3/2}$ transition is a continuous wave with a Gauss profile, and that of the coupling laser labeled as DL 2 operating at 776 nm related to the $5P_{3/2}-5D_{5/2}$ transition. The natural linewidths of the $5P_{3/2}$ and $5D_{5/2}$ states are approximately 6.0 MHz[18] and 0.67 MHz,[19] respectively. The probe laser is locked to $5S_{1/2}(F=2)-5P_{3/2}(F'=3)$ hyperfine transition by the saturated absorption spectroscopy method, while the coupling laser is scanned over the entire range of the excited states for the transition lines $5P_{3/2}-5D_{5/2}$; the frequency of the coupling laser is monitored with a wavelength meter (WS-7, HighFinesse). When the atoms are resonant with the fields of the coupling laser and the probe laser, the population of the $5S_{1/2}(F=2)$ state will deplete, due to the atoms excited to the $5D_{5/2}(F''=2,3,4)$ states decaying to the other ground state, $5S_{1/2}(F=1)$, by the intermediate states, $5P_{3/2}(F'=1,2)$. This phenomenon can be distinctly observed by monitoring the transmission of the probe laser. The advantage of this method is that the DROP spectroscopy has a flat background, at the same time, the spectral linewidth is narrowed due to the atomic coherence effect. Each laser's power can be controlled with a neutral-density plate (NDP). The polarization of the probe and coupling lasers can be controlled by the half-wave plate and quarter-wave plate introduced into the optical path. The quantum axis is along the direction of the probe laser. The vapor cell, 2.5 cm in diameter and 10 cm in length at room temperature, is placed in a μ-metal box to shield the stray magnetic field. The focused probe laser and the coupling laser beams in the center of the vapor cell are all about 100 μm. The transmission signal of the probe laser beam is detected by a Si photodiode detector (PDA36 A-EC, Thorlabs).

Considering the different hyperfine transition channels and hyperfine transition rules, the atoms of the ground state $5S_{1/2}(F=2)$ are excited to the $5D_{5/2}(F''=2,3,4)$ state via the intermediate state $5P_{3/2}$. With the scanning of the coupling laser around the entire range of $5P_{3/2}-5D_{5/2}$ transition while the probe laser is locked to $5S_{1/2}(F=2)-5P_{3/2}(F'=3)$ hyperfine transition, the transmittance peaks of the $5D_{5/2}(F''=2,3,4)$ state can be observed by monitoring the absorption of the probe laser beam, which is known as the typical DROP spectroscopy. The peaks are corresponding to $F''=4,3,2$ levels from left to right.

The absolute and relative amplitude of the peaks for the DROP spectra will be significantly influenced by the polarization combinations of the two lasers due to the different transition probabilities between different Zeeman levels. For a transition between two pure Zeeman levels (m_F and $m_{F'}$) of different hyperfine structures, the transition probability is given by[20]

$$\begin{aligned}
&\sigma_{m_F m_{F'}} \\
&= \langle F m_F | e\boldsymbol{r} | F m_{F'} \rangle \\
&= \langle J \| e\boldsymbol{r} \| J' \rangle (-1)^{2F'+J+I+m_F} \\
&\quad \times \sqrt{(2F+1)(2F'+1)(2J+1)} \\
&\quad \times \begin{pmatrix} F' & 1 & F \\ m_F & m_F & -m_{F'} \end{pmatrix} \\
&\quad \cdot \begin{Bmatrix} J & J' & 1 \\ F' & F & 1 \end{Bmatrix},
\end{aligned} \tag{1}$$

where $\langle J \| e\boldsymbol{r} \| J' \rangle$ is the reduced matrix element and will keep a constant for a hyperfine transition, and the value can be found in Ref. [21], I is the nuclear spin ($I=3/2$ for ^{87}Rb), J is the angular momentum, F represents the total angular momentum, and m_F stands for the magnetic sublevels of F states. Each F state has $(2F+1)$ degenerate m_F values. The primes on the quantum numbers correspond to the initial state where the atom resides. The quantities in brackets are the $3j$ symbol and in curled brackets are $6j$ symbols, which can be evaluated by Wolfram

Mathematica. The different sublevel transitions are driven by different laser beams, the sublevel transitions of $\Delta m_F = 0$, 1 and -1 are driven by π, σ^+ and σ^- polarized laser in one-photon transition. With the condition of that the quantum axis is along the direction of the laser transmission, the π, σ^+, σ^- polarized lasers represent the linearly polarized, right handed-circularly polarized and left-handed circularly polarized lasers, respectively.

The relative transition amplitudes of different transition peaks can then be quantitatively evaluated by $|\sigma_{m_F m_{F'}}|^2$, thus the transition probability from a given F, m_F level to any other F'', $m_{F''}$ level. Since there are a series of possible transition routes from the ground level to the upper level, each with its own weighted probability. By multiplying probabilities for the two transitions $(5S_{1/2} - 5P_{3/2})$ and $(5P_{3/2} - 5D_{5/2})$, we arrive at the two-photon transition probability for each allowed m_F to $m_{F''}$ level. Then, summing over all allowed transitions, we can obtain the transition probability between hyperfine states $\sum_{m_F - m_{F'}, m_{F'} - m_{F''}} (|\sigma_{m_F m_{F'}}|^2 |\sigma_{m_{F'} m_{F''}}|^2)$. The combinations of the laser beams can be divided into four groups, two linearly polarized, a linearly polarized and a circularly polarized, two same circularly polarized, two different circularly polarized. The transition probabilities for $5S_{1/2}(F = 2) - 5P_{3/2}(F' = 1, 2, 3) - 5D_{5/2}(F'' = 4, 3, 2)$ peaks with four combinations of the polarized laser beams are calculated and normalized by $F'' = 4$ of $\pi - \pi$ combination as, 1:0.34:0.32 for $\pi - \pi$ combination, 0.75:0.57:0.19 for $\pi - \sigma^+(\sigma^-)$ combination, 1.5:0.51:0.19 for $\sigma^+ - \sigma^+(\sigma^- - \sigma^-)$ combination, and 0.25:0.4:0.32 for $\sigma^+ - \sigma^-(\sigma^- - \sigma^+)$ combination, respectively.

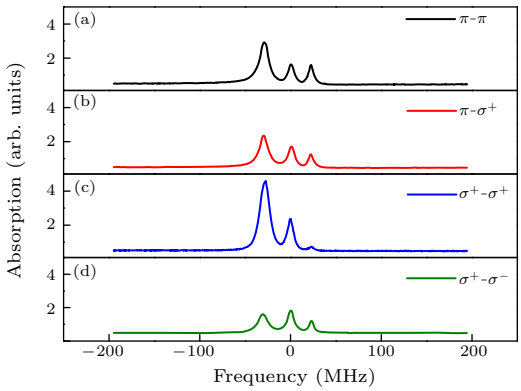

Fig. 2. The DROP spectra of ^{87}Rb atoms $5S_{1/2} - 5P_{3/2} - 5D_{5/2}$ with different polarization combinations of the laser beams. Here π represents the linearly polarized laser, σ^+ represents right-handed circularly polarized laser, and σ^- represents left-handed circularly polarized laser.

The experimental verification of the effect of different polarization combinations on the $5S_{1/2} - 5P_{3/2} - 5D_{5/2}$ transition of ^{87}Rb is shown in Fig. 2. The powers of the probe and coupling laser beams are 0.45 mW and 0.5 mW, respectively. Figure 2(a) shows the result of the two laser beams all with π linearly polarized, Fig. 2(b) is the situation of the probe laser which is π linearly polarized while the coupling laser is σ^+ right-handed circularly polarized, Fig. 2(c) is the result with all σ^+ right-handed circularly polarized, Fig. 2(d) is that the probe laser is σ^+ right-handed circularly polarized, and the coupling laser is σ^- left-handed circularly polarized.

We can find that the relative amplitudes of each of these peaks depend on the relative polarization orientations of the optical field as predicted by the theory. It can be clearly seen that the amplitudes of the $5D_{5/2}(F' = 4)$ peaks in the $\sigma^+ - \sigma^+$ case are much greater than those in the other cases. We choose the combination of the $\pi - \pi$ polarized laser beams for the following experiment since all the peaks have moderate amplitudes and can be resolved clearly.

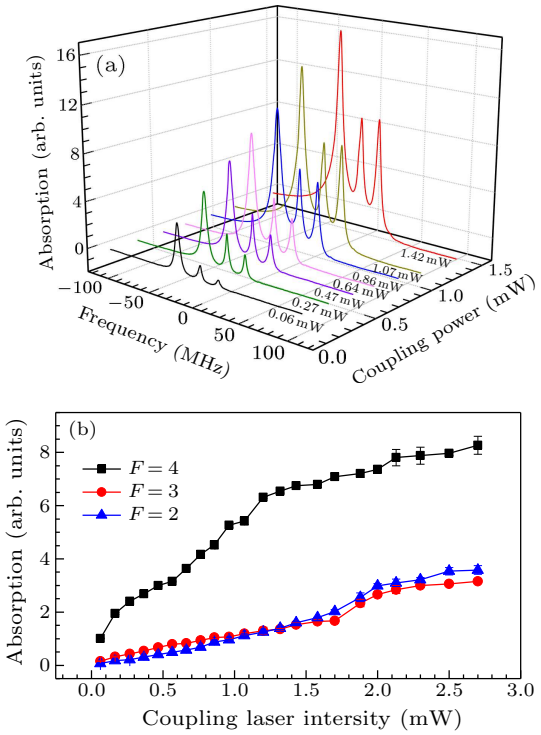

Fig. 3. (a) The DROP spectra of ^{87}Rb $5S_{1/2} - 5P_{3/2} - 5D_{5/2}$ transition with different coupling laser powers. (b) The peaks amplitude of the $5S_{1/2} - 5P_{3/2} - 5D_{5/2}$ transition of ^{87}Rb versus coupling laser power. The dots are the experimental results, the solid lines are the connection of the experimental results, and the errors are the standard deviation of three measurements.

We also investigate the dependence of the $5S_{1/2} - 5P_{3/2} - 5D_{5/2}$ transitions of ^{87}Rb atom on coupling laser powers, which is shown in Fig. 3(a). The power of the probe laser is 0.45 mW, while the powers of the coupling laser are 0.06, 0.27, 0.47, 0.64, 0.86, 1.07, and 1.42 mW measured by a power meter (S130C, Thorlabs). A distinct increase of the amplitude of the peaks is found with the coupling laser power. As noted in a previous report,[22] the DROP spectra for $4D_{3/2}$ and $4D_{5/2}$ show similar behavior for the power dependence. Meanwhile, as the power of the coupling

laser increases, the linewidth becomes larger due to the power broadening effect. In contrast, as can be seen in Fig. 3(b), different peaks of the $5D_{5/2}$ level exhibit dramatic variations as the coupling laser power changes. When the coupling laser power is weaker than 1.2 mW, the amplitude for the $5D_{5/2}(F = 3)$ peak is larger than the signals for the $5D_{5/2}(F = 2)$ level. However, as the laser power increases, the absorption amplitude becomes weaker than the other signal. This can be attributed to the strong cycling transition between the $5P_{3/2}$ and the $5D_{5/2}(F = 3)$ levels. The atoms in excited states can be spontaneously transferred to the $5S_{1/2}(F = 1)$ ground state through different paths, and each relative amplitude of the hyperfine states transition can be changed according to the laser power. When the coupling laser intensity is weak, while the strength of the cycling transition line $5P_{3/2} - 5D_{5/2}(F = 3)$ is very strong, the population of the intermediate state $5P_{3/2}$ is easily depleted for that cycling transition line, resulting in a large amplitude of the peak. However, when the intensity of the coupling laser is increased, the effect of the optical pumping for other transitions exceeds the saturation effect of the cycling transition. Therefore, we can observe the reverse of $5D_{5/2}(F = 2)$ when the coupling laser power exceeds 1.2 mW.

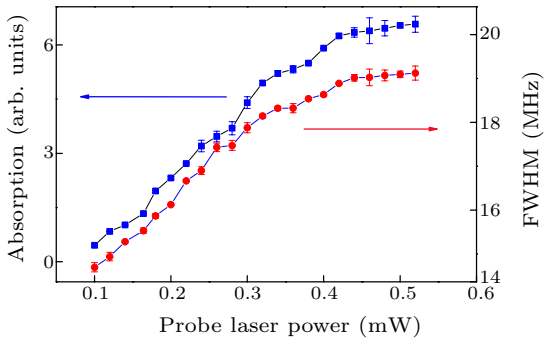

Fig. 4. The peak amplitude and full width at half maximum (FWHM) of the $5D_{5/2}(F'' = 4)$ hyperfine transition of ^{87}Rb with different probe laser powers. The dots are the experimental results. The solid lines are the connection of the experimental results, and the errors are the standard deviation of three measurements.

Lastly, the dependence of the $5S_{1/2} - 5P_{3/2} - 5D_{5/2}(F'' = 4)$ transitions of ^{87}Rb atom on probe laser powers is qualitatively studied, as shown in Fig. 4. The power of the probe laser ranges from 0.1 mW to 0.6 mW while the coupling laser power is kept at 1.1 mW. The amplitude and the FWHW both increase with the probe laser power due to the optical pumping effect.[23] The saturation effect is observed when the probe laser power exceeds 0.45 mW.

In conclusion, the high resolution DROP spectroscopy in a $5S_{1/2} - 5P_{3/2} - 5D_{5/2}$ ladder-type system of ^{87}Rb has been obtained. The polarization combinations and the power dependences of the two laser beams are investigated in theory and experiment. The absolute and relative amplitudes of the transition peaks are significantly affected by the polarization combinations of the two lasers due to the different transition probabilities between different Zeeman levels. The experimental results show a good agreement with the theoretical simulation. The research about the dependence of the DROP spectroscopy on the power of the coupling laser field shows that the amplitude of the transition peaks increases with the laser power, but the amplitude changes are not linear for the dramatic cycling transition. The variations of the DROP spectroscopy as the probe laser power changes show saturation behavior. This study gives a thorough perspective about the DROP spectroscopy, which will promote the development of the potential applications in precision measurement.

References

[1] Argence B, Chanteau B, Lopez O, Nicolodi D, Abgrall M, Chardonnet C, Daussy C, Darquié B, Coq Y L and Amy-Klein A 2015 *Nat. Photon.* **9** 456
[2] Riehle F 2017 *Nat. Photon.* **11** 25
[3] Zheng X, Sun Y R, Chen J J, Jiang W, Pachucki K and Hu S M 2017 *Phys. Rev. Lett.* **119** 263002
[4] Yan M, Luo P L, Iwakuni K, Millot G, Hänsch T W and Picqué N 2017 *Light: Sci. Appl.* **6** 17076
[5] Ding D S, Zhou Z Y and Shi B S 2012 *Chin. Phys. Lett.* **29** 024202
[6] Tsai C C, Bahns J T, Whang T J, Wang H, Stwalley W C and Lyyra A M 1993 *Phys. Rev. Lett.* **71** 1152
[7] Fleischhauer M, Imamoglu A and Marangos J P 2005 *Rev. Mod. Phys.* **77** 633
[8] Moon H S, Lee W K and Lee L 2004 *Appl. Phys. Lett.* **85** 3965
[9] Lee W K, Moon H S and Suh H S 2007 *Opt. Lett.* **32** 2810
[10] Moon H S, Lee W K and Suh H S 2009 *Phys. Rev.* A **79** 062503
[11] Wang J, Liu H F, Yang G, Yang B D and Wang J M 2014 *Phys. Rev.* A **90** 052505
[12] Yang B D, Zhao J Y, Zhang T C and Wang J M 2009 *J. Phys.* D **42** 085111
[13] Talker E, Stern L, Naiman A, Barash Y and Levy U 2017 *J. Phys. Commun.* **1** 055016
[14] Becerra F E, Willis R T, Rolston S L and Orozco L A 2008 *Phys. Rev.* A **78** 013834
[15] Cao S K, Fan P R, Zhang Y C, Wang L R, Xiao L T and Jia S T 2016 *Chin. Phys. Lett.* **33** 023201
[16] Wang L R, Zhang Y C, Xiang S S, Cao S K, Xiao L T and Jia S T 2015 *Chin. Phys.* B **24** 063201
[17] Li S H, Li Y H, Yuan J P, Wang L R, Xiao L T and Jia S T 2018 *Chin. Opt. Lett.* **16** 060203
[18] Ye J, Swartz S and Jungner P 1996 *Opt. Lett.* **21** 1280
[19] Grove T T, Sanchez-Villicana V, Duncan B C, Maleki S and Gould P L 1995 *Phys. Scr.* **52** 271
[20] Cheng H, Wang H M, Zhang S S, Xin P P, Luo J and Liu H P 2017 *Opt. Express* **25** 33580
[21] Shore B W 1990 *The Theory of Coherent Atomic Excitation* (New York: Wiley-Interscience)
[22] Noh H R and Moon H S 2009 *Phys. Rev.* A **80** 022509
[23] He Z S, Tsai J H, Chang Y Y, Liao C C and Tsai C C 2013 *Phys. Rev.* A **87** 033402